
Optical activity of $\text{Sn}_2\text{P}_2\text{S}_6$ crystals at the phase transition

Vlokh¹ R., Mys¹ O., Grabar² A. and Vysochanskii² Yu.

¹Institute of Physical Optics, 23 Dragomanov St., 79005 Lviv, Ukraine,
e-mail: vlokh@ifp.lviv.ua

²Institute for Solid State Physics and Chemistry, Uzhgorod National University,
54 Voloshyn St., 88000 Uzhgorod, Ukraine,
e-mail: inpcss@univ.uzhgorod.ua

Received: 24.11.2007

Abstract

Temperature dependence of optical activity in $\text{Sn}_2\text{P}_2\text{S}_6$ crystals has been studied in the course of proper ferroelectric phase transition. The electrogyration parameters of these crystals have been calculated. We have shown that the crystals under study might be referred to at least as one of the best electrogyration materials.

Keywords: $\text{Sn}_2\text{P}_2\text{S}_6$ crystals, optical activity, electrogyration

PACS: 78.20.Ek, 42.70.Jk, 78.20.Hp, 77.80.Bh

UDC: 535.51

Introduction

$\text{Sn}_2\text{P}_2\text{Se}_6$ crystals belong to the family of ferroelectric-semiconducting $\text{Sn}_{2x}\text{Pb}_{2(1-x)}\text{S}_{6y}\text{Se}_{6(1-y)}$ crystals (see, e.g., [1]). These crystals are transparent in the spectral range of $0.53\text{--}8.0\ \mu\text{m}$. They manifest a proper ferroelectric phase transition at $T_c = 337\ \text{K}$, with the change of point symmetry group $2/mFm$. The crystals are interesting from the point of view of their excellent electrooptic [2, 3] piezooptic [4, 5], acoustooptic [6, 7] and photorefractive [8, 9] properties. It has also been found that $\text{Sn}_2\text{P}_2\text{S}_6$ crystals reveal very high electrooptic ($r_{11} = 174\ \text{pm/V}$) and acoustooptic ($M_2 = (1.7 \pm 0.4) \times 10^{-12}\ \text{kg/s}^3$) figures of merit. Besides, the crystals under consideration can be efficiently used for optical photorefractive storage in the near infrared. Unfortunately, the results on the optical activity in $\text{Sn}_2\text{P}_2\text{S}_6$ crystals are still absent, though the gyration effect can essentially affect at least the process of photorefractive diffraction.

On the other hand, a principal possibility has been recently shown for realization of planar waveguides based on $\text{Sn}_2\text{P}_2\text{S}_6$ [10], thus suggesting that the crystals can be utilized in the integrated optics. Up to now, electrogyration effect is not used in practical optoelectronics, whereas the angles of electrically induced optical rotation accessible at high operating voltages are quite small for the most of materials. For example, the highest

value of electrogyration coefficient has been revealed maybe for the lead germanate crystals doped with Cr ions ($\gamma_{33} = 31 \text{ pm/V}$) at the temperature of phase transition [11]. Nonetheless, practical utilizations of any material at the temperatures close to the Curie one are complicated by instabilities imposed by these conditions. Let us note that some semiconductor crystals show very good electrogyration parameters in the range of their exciton absorption [12, 13], however the corresponding liquid-helium temperatures hinder utilization of this property. Besides, the electrogyration effect exhibits a number of advantages, when compare with the electrooptic one. In particular, one can remind larger number of crystals that possess the former effect (the linear electrogyration effect is not forbidden in centrosymmetric crystals, contrary to the Pockels effect), as well as a possibility for direct polarization modulation of light.

Basing on a natural assumption that electrogyration and electrooptic coefficients of any material should be of the same order of magnitude (see, e.g., [14]) and on the fact that $\text{Sn}_2\text{P}_2\text{S}_6$ crystals are proper ferroelectrics (i.e., changes in both the optical birefringence and the optical activity at the phase transition are directly coupled with spontaneous electric polarization), one can roughly estimate the values of gyration and electrogyration coefficients. Such the estimations yield in very high values of optical rotation in single-domain state at the room temperature ($\sim 100 \text{ deg/mm}$). This should mean that switching of enantiomorphous domains (the value of the coercive field is $15 - 92 \text{ V/mm}$, depending upon pre-illumination of samples [15]) would lead to 90° reversal of light polarization plane at reasonably low electric fields. Furthermore, the electrogyration rotation of the polarization plane by the angles $\sim 10 \text{ deg/mm}$ should possibly appear at the electric fields as small as $\sim 100 \text{ V/mm}$. It is worth noticing that such a large value of electrogyration has never been observed before. Hence, the goal of the present work is experimental studies of the electrogyration effect in $\text{Sn}_2\text{P}_2\text{S}_6$ crystals undertaken in order to verify our preliminary theoretical estimates.

Experimental

Since the $\text{Sn}_2\text{P}_2\text{S}_6$ crystals belong to centrosymmetric symmetry group in the paraelectric phase, the natural optical activity above T_c is forbidden by the symmetry. At the same time, the gyration can exist below the phase transition temperature. Moreover, the domains with the opposite signs of spontaneous electric polarization should be enantiomorphous, because the centre of symmetry is lost at the phase transition. The gyration tensor g_{ij} for the point symmetry group m , written in the crystallographic frame of reference, has the following form:

$$g_{ij} = \begin{array}{c|ccc} & k_1 & k_2 & k_3 \\ \hline \rho_1 & 0 & g_{12} & 0 \\ \rho_2 & g_{12} & 0 & g_{23} \\ \rho_3 & 0 & g_{23} & 0 \end{array} . \quad (1)$$

In the eigen frame of reference it may be rewritten as

$$g_{ij} = \begin{array}{c|ccc} & k_1 & k_2 & k_3 \\ \hline \rho_1 & (g_{12}^2 + g_{23}^2)^{1/2} & 0 & 0 \\ \rho_2 & 0 & 0 & 0 \\ \rho_3 & 0 & 0 & -(g_{12}^2 + g_{23}^2)^{1/2} \end{array}, \quad (2)$$

where ρ_i is the angle of specific rotation of light polarization plane and k_j the light wave vector. The angle of rotation of the gyration surface around the b axis is defined by the relation

$$\tan \xi_b = \frac{g_{23}}{g_{12}}. \quad (3)$$

The scalar gyration parameter in the crystallographic frame of reference may be presented as (see Fig. 1)

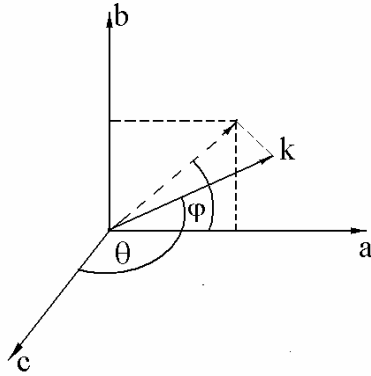


Fig. 1. Cartesian and polar frames of reference. The Cartesian frame of reference is very close to crystallographic one, with the only difference that the axes a and c of the latter are slightly nonorthogonal.

$$G = g_{ij}l_i l_j = \rho n_m \lambda / \pi = g_{12} \sin^2 \Theta \sin 2\varphi + g_{23} \sin 2\Theta \sin \varphi, \quad (4)$$

where $l_1 = \sin \Theta \cos \varphi$, $l_2 = \sin \Theta \sin \varphi$, $l_3 = \cos \Theta$ ($1 \leftrightarrow a$, $2 \leftrightarrow b$ and $3 \leftrightarrow c$), n_m is the mean refractive index and λ the light wavelength.

$\text{Sn}_2\text{P}_2\text{S}_6$ crystals are optically biaxial. For the room temperature and $\lambda = 632.8 \text{ nm}$, their plane of optic axes is parallel to the b axis and is rotated by $\sim 45^\circ$ with respect to the a and c axes (see [16]). Under the same conditions, the angle between the optic axes is equal to $\sim 90^\circ$. In such a case the optical rotation should manifest itself when the light propagates along one of the optic axes (Fig. 2).

As one can see from Fig. 2, the optical rotation should have the same magnitude and the opposite signs when the light propagates along different optic axes. Taking into account the orientation of the plane of optic axes (the angle between the plane of optic axes and the a axis being equal to α), one can derive the relations for the angles φ and Θ :

$$\varphi = \arcsin \left[\frac{\cos V}{\sqrt{1 - \sin^2 V \sin^2 \alpha}} \right], \quad (5)$$

$$\Theta = \arccos[\sin \alpha \sin V], \quad (6)$$

where $2V$ denotes the angle between the optic axes. Basing on Eqs. (5) and (6), we rewrite Eq. (4) as

$$G = g_{ij}l_i l_j = \rho n_m \lambda / \pi =$$

$$= g_{12} \sin^2 \left\{ \arccos[\sin \alpha \sin V] \right\} \sin \left\{ 2 \arcsin \left[\frac{\cos V}{\sqrt{1 - \sin^2 V \sin^2 \alpha}} \right] \right\} +,$$

$$g_{23} \sin \left\{ 2 \arccos[\sin \alpha \sin V] \right\} \left\{ \frac{\cos V}{\sqrt{1 - \sin^2 V \sin^2 \alpha}} \right\}$$
(7)

For the room temperature and the wavelength of $\lambda = 632.8 \text{ nm}$ we have $\alpha = 45 \text{ deg}$, $V = 45 \text{ deg}$, $\varphi = 54.74 \text{ deg}$ and $\Theta = 57.23 \text{ deg}$. For the conditions specified above and the light propagation along the optic axis one can modify Eq. (7) to the following form:

$$G = g_{ij}l_i l_j = \rho \lambda n_m / \pi = 0.705 g_{12} + 0.707 g_{23} \approx 0.7(g_{12} + g_{23}).$$
(8)

Following from the said above, the optical activity in $\text{Sn}_2\text{P}_2\text{S}_6$ crystals can be measured with a direct technique for the rotation of polarization plane and the light propagating along one of the optic axes. However, there is a difficulty peculiar for low-symmetry $\text{Sn}_2\text{P}_2\text{S}_6$ crystals: the eigen frame of reference for the gyration tensor does not coincide neither with the eigen frame of reference for the optical indicatrix ellipsoid nor with the crystallographic one. Moreover, the orientation of the plane of optic axes, the angle between the optic axes and the angle of rotation of the gyration surface around the b axis can show different temperature behaviours. For example, the angle between the optic axes decreases approximately by $\sim 10 \text{ deg}$, when the temperature changes from the room one to T_c . At the same time, the plane of optic axes also rotates, though approximately by $\sim 12 \text{ deg}$ [17]. Nevertheless, these rotations do not effect essentially the form of Eq. (8), so that it remains approximately valid for the whole interval between the room temperature and T_c . However, serious problems arise within the mentioned technique if it is necessary to change the sample temperature or the wavelength of optical radiation. The location of the plane of optic axis changes if these parameters are

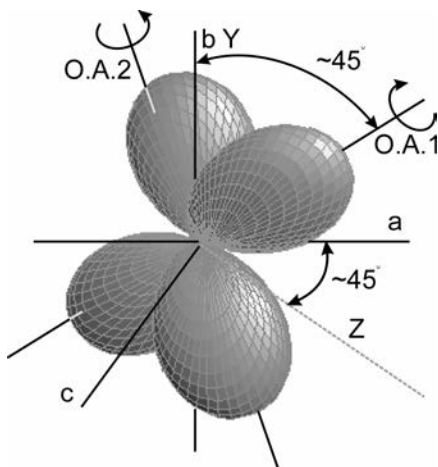


Fig. 2. Shape of the gyration surface for $\text{Sn}_2\text{P}_2\text{S}_6$ crystals in crystallographic frame of reference and outlets of the optic axes at the room temperature.

changing, and the same is true of the angle between the optic axes. Thus, at each temperature the sample should be rotated by some angle and the corresponding change in the optical path should properly be taken into account.

The polarimetric experimental set up used by us is shown in Fig. 3,a. He-Ne laser with the wavelength of radiation 632.8nm was used as a light source. The azimuth of the incident light was chosen in such a way that it always remained perpendicular to the plane of incidence during the temperature changes (see Fig. 3,b). This prevented appearance of elliptically polarized light inside the sample at the oblique incidence of light on the sample. The sample with the faces perpendicular to one of the optic axis was placed into a heating stage with the temperature stabilization not worse than 0.1K. The thickness of the sample was $d_0 = 1.68\text{mm}$. A furnace with windows of wide aperture was mounted on a rotation stage that allowed rotations of the furnace with the sample by required angles defined by the directions of optic axis at each temperature. The effective sample thickness was recalculated using the formula

$$d = \frac{d_0}{\cos \left[\arcsin \left(\frac{\sin \beta}{n_m} \right) \right]}, \quad (9)$$

where β is the angle of incidence and $n_m = 3.0256$. We checked the sample for availability of enantiomorphous domains while scanning the laser beam across the sample

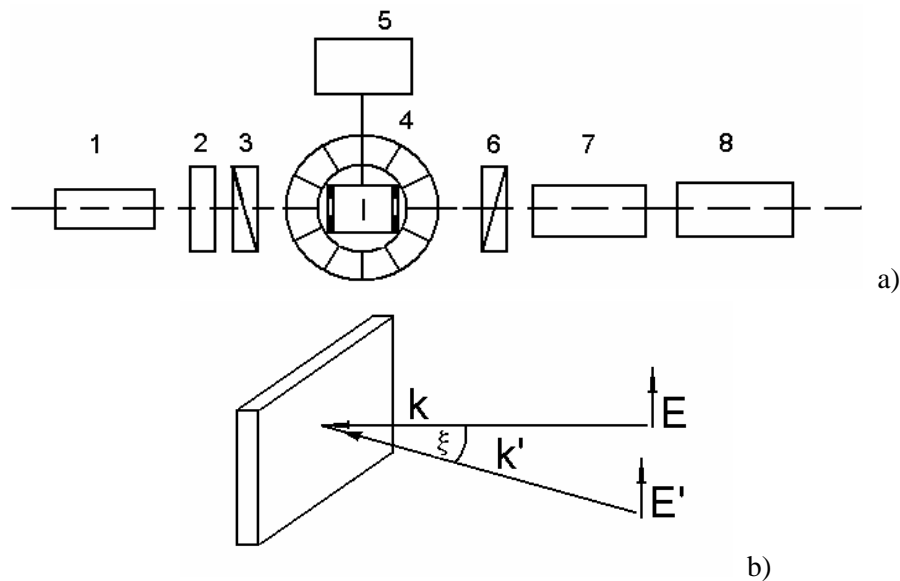


Fig. 3. (a) Scheme of polarimetric set-up for studying temperature dependence of the optical activity in $\text{Sn}_2\text{P}_2\text{S}_6$ crystals: 1 – He-Ne laser, 2 – quarter-wave plate, 3 and 6 – polarizers, 4 – rotation stage with furnace and sample, 5 – power supply, 7 – photomultiplier with oscilloscope 8.

(b) Sample orientation: k and k' correspond to different temperatures ($T \neq T'$).

surface at the room temperature and measuring the optical rotation angles. The sample was proven to be single-domain and, moreover, we did not observe any inhomogeneous distribution of optical activity over the sample square.

Results and discussion

The conoscopic fringes appearing in case when the light propagates along one of the optic axes in $\text{Sn}_2\text{P}_2\text{S}_6$ crystals are presented in Fig. 4.

The temperature dependence of the optical rotation power is shown in Fig. 5. As one can see, the optical rotation decreases when the temperature approaches the Curie point at heating. The polarimetric measurements in the vicinity of T_c have been complicated by a light scattering, which is probably caused by some intermediate state appearing under the temperature stabilization near T_c (see, e.g., [1]). The critical exponent governing the temperature dependences of both the optical rotation and the order parameter ($\rho \sim P_s \sim (T_c - T)^\beta$) is calculated to be equal $\beta = 0.43$.

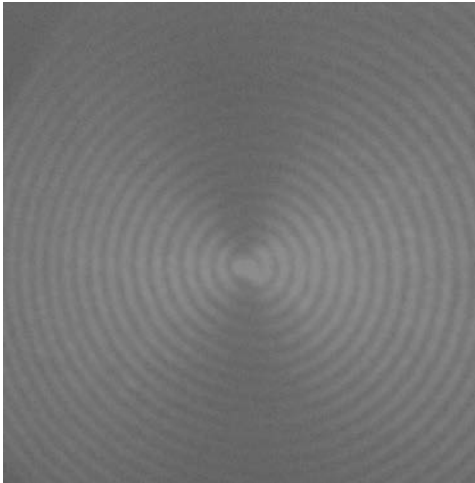


Fig. 4. Conoscopic fringes peculiar for the light propagation along one of the optic axes in $\text{Sn}_2\text{P}_2\text{S}_6$ crystals.

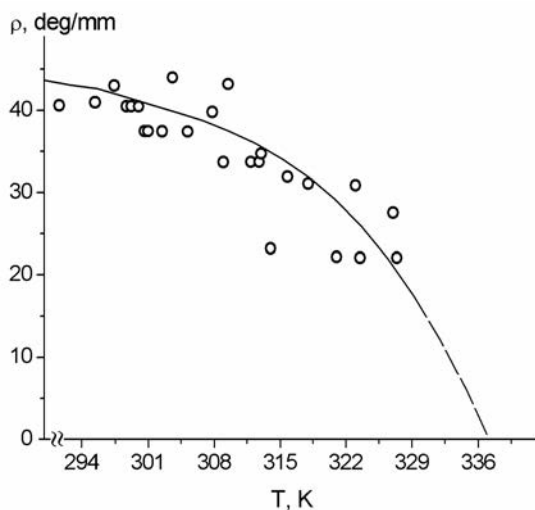


Fig. 5. Temperature dependence of specific optical rotation in $\text{Sn}_2\text{P}_2\text{S}_6$ crystals for the case of light propagation along one of the optic axes ($\lambda = 632.8 \text{ nm}$).

The optical rotation has quite a large value ($\rho = (44.3 \pm 1.5) \text{ deg/mm}$) at the room temperature. It is possible that the optical rotation characteristic of the propagation direction corresponding to the apex of the gyration surface (see Fig. 2) should be still larger. Considering the optical activity and the electrogyration effect induced by spontaneous polarization, one can write the relations

$$\Delta g_{ij} = \gamma_{ijk} P_k^s, \quad (10)$$

$$\Delta g_{12} = \gamma_{61}^* P_1^s, \quad (11)$$

$$\Delta g_{23} = \gamma_{41}^* P_1^s, \quad (12)$$

$$g_{12} + g_{23} = \rho \lambda n_m / 0.7 \pi = (\gamma_{61}^* + \gamma_{41}^*) P_1^s \quad \text{at } T = 293 \text{ K}, \quad (13)$$

where γ_{41}^* and γ_{61}^* are the electrogyration coefficients for the paraelectric phase, defined in the units of reciprocal spontaneous polarization, and P_s is the spontaneous polarization. The calculations have yielded very high values of the effective gyration coefficient ($(g_{12} + g_{23})_{T=293K} = (6.7 \pm 0.2) \times 10^{-4}$) and the circular birefringence ($\Delta n_c = (g_{12} + g_{23}) / n_m = (2.22 \pm 0.08) \times 10^{-4}$).

Dependence of the optical rotatory power on the spontaneous polarization is shown in Fig. 6, where the temperature dependence of the polarization has been taken from [17].

It follows from the theoretical considerations (see also Eq. (13)) that the dependence should be linear. The effective electrogyration coefficient is determined as $\gamma_{61}^* + \gamma_{41}^* = (g_{12} + g_{23}) / P_s = (4.3 \pm 0.1) \times 10^{-3} \text{ m}^2/\text{C}$. Using this value, which should be independent of temperature, it is possible to calculate the effective electrogyration coefficients defined in the reciprocal units of electric field. The latter are equal to

$$(\gamma_{61} + \gamma_{41})_{T=T_c} = (\gamma_{61}^* + \gamma_{41}^*) \epsilon_0 (\epsilon_3^{T=T_c} - 1) \approx 11.4 \times 10^{-10} \text{ m/V} \quad \text{at } T = T_c, \quad (14)$$

and

$$(\gamma_{61} + \gamma_{41})_{T=293K} = (\gamma_{61}^* + \gamma_{41}^*) \epsilon_0 (\epsilon_3^{T=293K} - 1) \approx 0.4 \times 10^{-10} \text{ m/V} \quad \text{at } T = 293 \text{ K}, \quad (15)$$

where we have made use of the parameters $\epsilon_3^{T=T_c} = 3 \times 10^4$ and $\epsilon_3^{T=293K} \approx 10^3$ [17]. These values are very high, probably, even the highest among the electrogyration coefficients ever found. On the basis of Eqs. (14) and (15) one can also estimate the angle of electrically induced optical rotation. For the room temperature, the wavelength of $\lambda = 632.8 \text{ nm}$ and the electric field and light wave vector directions parallel to the optic axis, this angle is equal to $\sim 0.34 \text{ deg}$ (at $U = 100 \text{ V}$), while at $T = T_c$ it reaches $\sim 10 \text{ deg}$ at the same voltage.

Another peculiarity of optical activity in the Sn₂P₂S₆ ferroelectrics is that different orientation states have the opposite signs of optical rotation, though they do not differ in the refractive indices. Hence, the switching of ferroelectric domain structure would lead

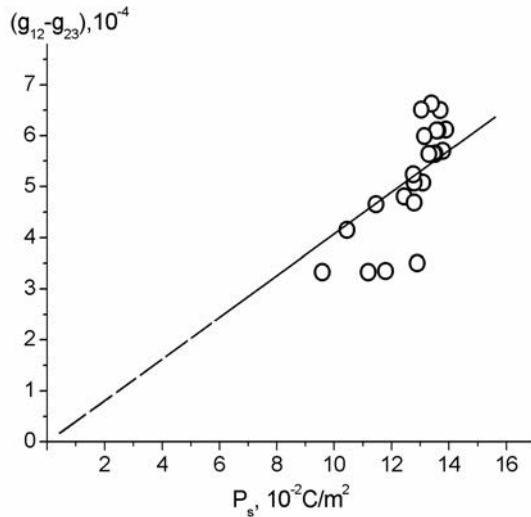


Fig. 6. Dependence of optical rotatory power on the spontaneous polarization for $\text{Sn}_2\text{P}_2\text{S}_6$ crystals.

to the optical activity changes as large as $\rho \approx 90 \text{ deg/mm}$, if only the electric field $\sim 184 \text{ V/mm}$ is applied along the direction parallel to P_s . This prominent property of $\text{Sn}_2\text{P}_2\text{S}_6$ crystals may be used for electromagnetic mode conversion and visualisation of the domain structure.

Conclusions

The main conclusion following from the present work is that the electrogyration effect can achieve quite large values, thus allowing its utilization at relatively low operative voltages. The electrogyration coefficient in the $\text{Sn}_2\text{P}_2\text{S}_6$ crystals under test is equal to $\sim 10^{-10} \text{ m/V}$, whereas for the most of compounds studied previously it is of the order of $\sim 10^{-12} \text{ m/V}$. We also show that, due to very high value of natural optical activity ($\rho = (44.3 \pm 1.5) \text{ deg/mm}$), switching of enantiomorphous ferroelectric domains in $\text{Sn}_2\text{P}_2\text{S}_6$ crystals can be used for conversion of electromagnetic modes and visualisation of the domain structure.

References

1. Vysochanskii YM, Janssen T, Currat R, Folk R, Banys J, Grigas J and Damulionis V Phase transitions in ferroelectric phosphorous chalcogenide crystals. Vilnius: Vilnius University Publishing House (2006).
2. Vlokh RO, Vysochanskii YuM, Grabar AA, Kityk AV and Slivka VYu, 1991. Electrooptic effect in $\text{Sn}_2\text{P}_2\text{S}_6$ ferroelectrics. *Izv. Akad. Nauk SSSR, Ser. Neorg. Mater.* **27**: 689–692.
3. Haertle D, Caimi G, Haldi A, Montemezzani G, Günter P, Grabar AA, Stoika IM and Vysochanskii YuM, 2003. Electro-optical properties of $\text{Sn}_2\text{P}_2\text{S}_6$. *Opt. Commun.* **215**: 333–343.
4. Mys O, Martynyuk-Lototska I, Grabar A, Vysochanskii Yu and Vlokh R, 2006.

- Piezooptic coefficients and acoustic wave velocities in $\text{Sn}_2\text{P}_2\text{S}_6$ Crystals. Ukr. J. Phys. Opt. **7**: 124–128.
5. Mys OG, Martynyuk-Lototska IYu, Grabar AA, Vysochanskii YuM and Vlokh RO, 2007. Piezooptic coefficients of $\text{Sn}_2\text{P}_2\text{S}_6$ crystals. Ferroelectrics. **352**: 171-175.
 6. Martynyuk-Lototska IY, Mys OG, Grabar AA, Stoika IM, Vysochanskii YuM and Vlokh RO, 2007. Highly efficient acoustooptic diffraction in $\text{Sn}_2\text{P}_2\text{S}_6$ crystals. Ukr. J. Phys. Opt. **8**: 78–82
 7. Martynyuk-Lototska IYu, Mys OG, Grabar AA, Stoika IM, Vysochanskii YuM and Vlokh R, 2008. Highly efficient acoustooptic diffraction in $\text{Sn}_2\text{P}_2\text{S}_6$ crystals. Appl. Opt. **47** (to be published).
 8. Odoulov SG, Shumelyuk AN, Hellwig U, Rupp R, Grabar AA and Stoyka IM, 1996. Photorefraction in tin hypthiodiphosphate in the near infrared. J. Opt. Soc. Am. B **13**: 2352–2360.
 9. Jazbinsek M, Montemezzani G, Gunter P, Grabar AA, Stoika IM and Vysochanskii YM, 2003. Fast near-infrared self-pumped phase conjugation with photorefractive $\text{Sn}_2\text{P}_2\text{S}_6$. J. Opt. Soc. Am. B. **20**: 1241–1256.
 10. Guarino A., Jazbinsek M, Herzog C, Degl'Innocenti R, Poberaj G, Gunter P, 2006. Optical waveguides in $\text{Sn}_2\text{P}_2\text{S}_6$ by low fluency MeV He^+ ion implantation. Opt. Express. **14**: 2344–2358.
 11. Adamenko D, Klymiv I, Duda V M., Vlokh R and Vlokh O, 2007. Electrically and magnetically induced optical rotation in $\text{Pb}_5\text{Ge}_3\text{O}_{11}:\text{Cr}$ crystals at the phase transition. 1. Electrogyration effect in $\text{Pb}_5\text{Ge}_3\text{O}_{11}:\text{Cr}$. Ukr. J. Phys. Opt. **8**: 42–53.
 12. Akhmanov SA, Zhdanov BV, Zheludev NI, Kovrigin NI and Kuznetsov VI, 1979. Nonlinear optical activity in crystals. Pisma Zhurn. Eksp. Teor. Fiz. **29**: 294–298.
 13. Zheludev NI, Karasev VYu, Kostov ZM and Nunuparov MS, 1986. Giant exciton resonance in nonlinear optical activity. Pisma Zhurn. Eksp. Teor. Fiz. **43**: 578–581.
 14. Vlokh O.G. Spatial dispersion phenomena in parametric crystal optics. Lviv: Vyshcha Shkola, (1984).
 15. Risak VM, Mayor MM, Vysochanskii YuM, Gurzan MI and Slyvka VYu, 1988. Photoelectret state and pyroelectric parameters stabilization in $\text{Sn}_2\text{P}_2\text{S}_6$ crystals. Ukr. J. Phys. **33**: 1740–1744.
 16. Haertle D, Guarino A, Hajfler J, Montemezzani G and Günter P, 2005. Refractive indices of $\text{Sn}_2\text{P}_2\text{S}_6$ at visible and infrared wavelengths. Optics Express. **13**: 2047–2057.
 17. Slyvka V.Yu. and Vysochanskii Yu. M. Ferroelectrics of $\text{Sn}_2\text{P}_2\text{S}_6$ family. Properties around the Lifshitz point. Uzhgorod: Zakarpattia (1994).